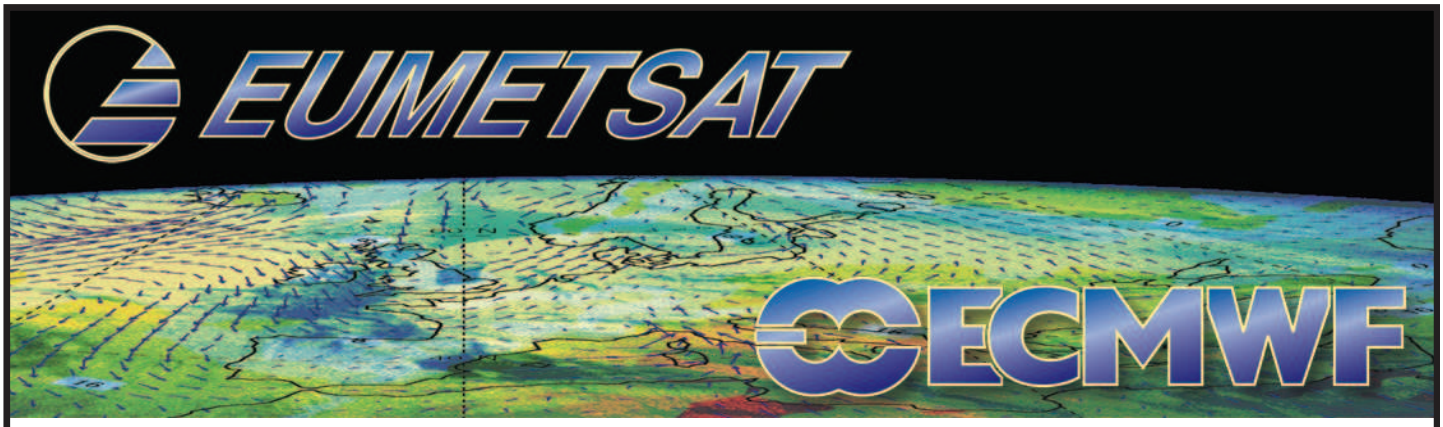

EUMETSAT/ECMWF Fellowship Programme
Research Report No. 21

Assimilation of radiance products from geo-stationary satellites: 1-year report

Cristina Lupu and Anthony McNally

January 2011

Series: EUMETSAT/ECMWF Fellowship Programme Research Reports

A full list of ECMWF Publications can be found on our web site under:
http://www.ecmwf.int/publications/

Contact: library@ecmwf.int

European Centre for Medium Range Weather Forecasts
Shinfield Park, Reading, RG2 9AX, England

1 Executive summary

This past year, following the replacement of GOES-12 by GOES-13 on 14th April 2010 and the replacement of MTSAT-1R by MTSAT-2 on 11th August 2010, work has been directed towards incorporating Clear Sky Radiances (CSR) from GOES-13 and MTSAT-2 on the operational ECMWF system. The maintenance of the geostationary network has been adapted to the assimilation of CSR from GOES-13 (with cycle 36r1) and MTSAT-2 (with cycle 36r4) and currently, CSR products from Meteosat-7/9, MTSAT-2 and GOES-11/13 are operationally assimilated at ECMWF. Routine monitoring and assessement of CSR from Meteosat-7/9 and GOES-11 show that geostationary CSR remain healthy in operations. This report gives an overview of the assimilation strategy of CSR from GOES-13 and MTSAT-2 and summarizes the results of monitoring and assimilation experiments performed to asses the impact of new CSR data sets on analysis and forecast quality. The main findings are as follows.

- An evaluation of data from GOES-13 has demonstrated that the radiances have reduced biases relative to data from GOES-12. This improved data quality is believed to be a result of significant improvements in instrument design. GOES-13 successfully replaced GOES-12 in ECMWF operations on 29 April 2010.
- An evaluation of data from MTSAT-2 has confirmed that the radiances are of very similar quality to those from MTSAT-1R. MTSAT-2 successfully replaced MTSAT-1R in ECMWF operations on 25 January 2011.
- During the evaluations of GOES-13 and MTSAT-2 it has again been confirmed that GEO radiance data enhance the quality of the ECMWF analysis and improve the fit to other independent observations (satellite and conventional). The impact of GEO radiances on headline forecast measures remains rather small.

The second stage of this study involves the use of all-sky radiance product (ASR-which are radiances averaged over segments of 16x16 pixels) from Meteosat-9 SEVIRI observations. The overcast cloudy scheme used operationally at ECMWF to directly assimilate cloud-affected infrared radiances from AIRS/IASI and HIRS polar orbiter data was extended to make use of the all-sky radiance products produced by EUMETSAT from Meteosat-9 SEVIRI data. The preliminary results of this study are:

- The ECMWF analysis system has been successfully extended to assimilate cloud affected radiance observations from SEVIRI.
- Cloud parameters (fraction and height) derived from the MET-9 SEVIRI ASR data inside the ECMWF 4D-Var agree extremely well with independent pixel-by-pixel estimates from EUMETSAT processing.
- Overcast SEVIRI radiances have been shown to provide information on temperature and humidity in addition to that provided by the clear-sky observations.

The main objective of this study is to extend the humidity tracing capability, previously demonstrated only in clear sky, to cloudy regions, to obtain an all-sky constraint the atmospheric wind field with geostationary radiances. The focus for the coming months is to work on assimilation of Meteosat-9 overcast cloudy data in addition to the clear-sky radiances from the two water-vapour channels currently operational assimilated. The extra cloudy data retained should cover the areas where clear sky radiances are not available. As part of this

work, we will quantify the impact of the new data set (CSR+overcast) on the wind analysis and compare with AMVs impact (specifically the height assignment of winds inferred from moving water vapour structures). It is hoped that this analysis will help to understand some of the issues associated with AMVs in terms of bias and error characterization as well as the underlying assumption that the motion of the tracked features can help to characterize the atmospheric wind field.

2 Monitoring and assimilation experiments with GOES-13 CSR

On 14 April 2010, GOES-13 replaced GOES-12 and has been declared the operational GOES-East in the NOAA Geostationary Operational Environmental Satellite (GOES) constellation. Currently, the GOES system consists of GOES-13 operating as GOES-East in the eastern part of the constellation at 75.5^o west longitude, and GOES-11 operating as GOES-West at 135^o west longitude. In addition, GOES-12 was repositioned at 60^o west longitude and provide coverage for South America since June 2010.

GOES-13 carries instruments (imager and sounder) similar to those on GOES-12, but the new spacecraft, equipped with an improved battery, allows it to operate through eclipse periods. Images have improved navigation, registration and radiometric accuracy. Clear sky radiances from GOES-13 have been produced by the Cooperative Institute for Meteorological Satellite Studies (CIMSS, Madison, USA) and have been received at ECMWF in near real-time since February 2010. The GOES-13 CSR data are derived for the water vapor channel or, channel 2 at 6.7μm and for the three infrared channels (IR) at 3.9μm (channel 1), 10.7μm (channel 3) and 13.3μm (channel 4).

2.1 GOES-13 CSR: monitoring experiments

Before a new observation is introduced to the assimilation system, initial monitoring of the background departures is undertaken. The GOES-13 CSR have been monitored initially offline from 2 to 28 February 2010 and from 16 March 2010 to 28 April 2010 they were passively monitored in the ECMWF operational assimilation system (cycle 36r1 of the Integrated Forecasting System). Figures 1 and 2 show a one month (2-28 February 2010) time series of analysis and background departure statistics of GOES-13 CSR for the WV (Fig. 1) and IR at 10.7μm channels (Fig. 2), respectively. The O-B (observations minus background) shows a mean departure of about -0.38 K for the WV channel and -1.04 K for the IR (10.7μm) channel. The O-A (observations minus analysis) are smaller than O-B, hence the analysis matches the observations better than does the background. After the variational bias correction (Dee, 2004) is applied the bias in the innovations (O-B) is close to zero in the WV channel and reduced in the IR channel 3. Results of monitoring experiments shows a good consistency between GOES-12 and GOES-13 data.

The quality of the GOES-13 data has been also investigated by comparison with data from GOES-12. Figure 3 shows time series of mean departure and standard deviation of GOES-12 (solid) and GOES-13 (solid with symbols) observed brightness temperature (in degrees K) minus the corresponding model first guess (blue) and analysis (red) estimates for the water vapor channel at 6.7μm from 2 to 28 February 2010. Side-by-side comparison of the two sets of data (Figure 3) showed that mean analysis and background departure statistics are reduced for GOES-13 data. The similarity of the standard deviation of the background and analysis departures for the GOES-13 and GOES-12 data indicates that in the water vapour channel the two sets of the data have a similar level of noise.

Histograms for the background and analysis departures for the WV channel of the GOES-13 are shown in Fig. 4 alongside histograms for the WV channel of the GOES-12. The analysis fit in the Northern Hemisphere

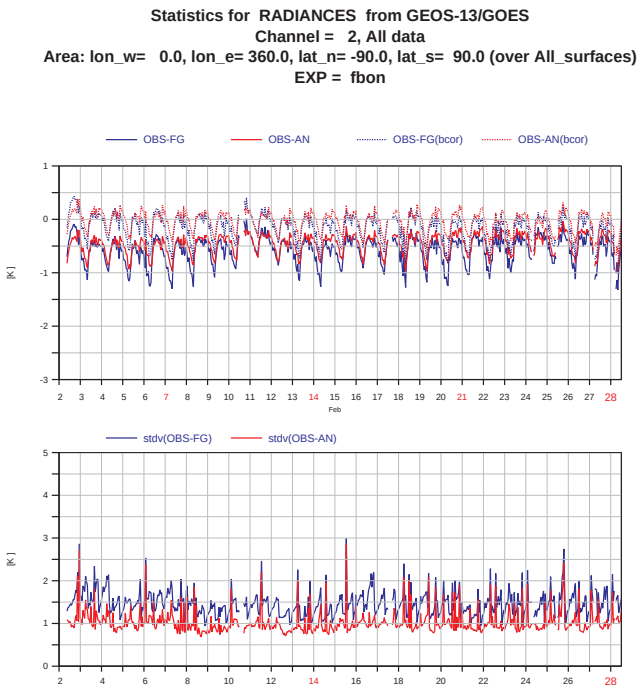

Figure 1: Time series of first-guess and analysis departure statistics, in K, for the off-line passive monitoring of GOES-13 WV-channel (6.7μm) over the period 2 to 28 February 2010.

has a standard deviation of about 1.05 K for GOES-13 and 0.91 for GOES-12, while the background departure standard deviation is 1.36 K for GOES-13 and 1.25 K for GOES-12. Results over Tropics and Southern hemisphere, not shown here, indicated also that the GOES-13 data are of very similar quality to the GOES-12 data.

Following these results it has been decided to proceed with assimilation experiments to assess the impact of the CSR from GOES-13 on analysis and forecast quality. The switch from passive to active was achieved via a blacklist change on 29 April 2010.

2.2 GOES-13 CSR: assimilation experiments

This section gives first a brief overview of the main components of GOES-13 CSR assimilation, namely the channel selection, data thinning, quality control, bias correction and presents the assimilation experiments realised in order to introduce GOES-13 WV CSR into the operational analysis. The current setting follows the previous one used for GOES-12 CSR.

GOES-13 CSR from the WV-channel were selected for the operational implementation while the CSR data from atmospheric window channel (10.7μm) which have contributions from the surface was used for quality control, but not for assimilation. To check the quality of the observations, the measured CSR (represented as a vector $\mathbf{y}$) are compared against the background state equivalent to the observations, $\boldsymbol{H}(\mathbf{x}_b)$, where $\boldsymbol{H}$ stands for the observation operator. The observation is rejected if the absolute departure of the observation from the calculated values exceeds a threshold around 6 K. The calculation of the departures between model first-guess and observations is useful to identify any type of gross errors in the observations.

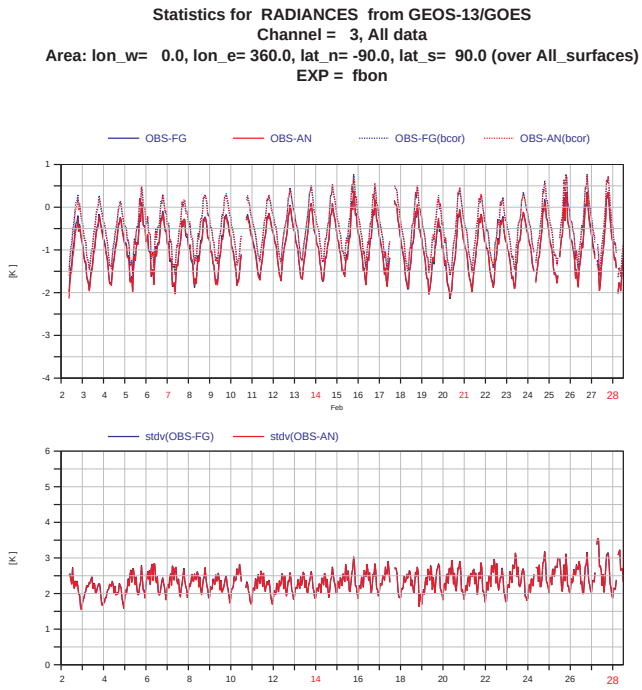

Figure 2: Time series of first-guess and analysis departure statistics, in K, for the off-line passive monitoring of GOES-13 window channel (10.8μm) over the period 2 to 28 February 2010.

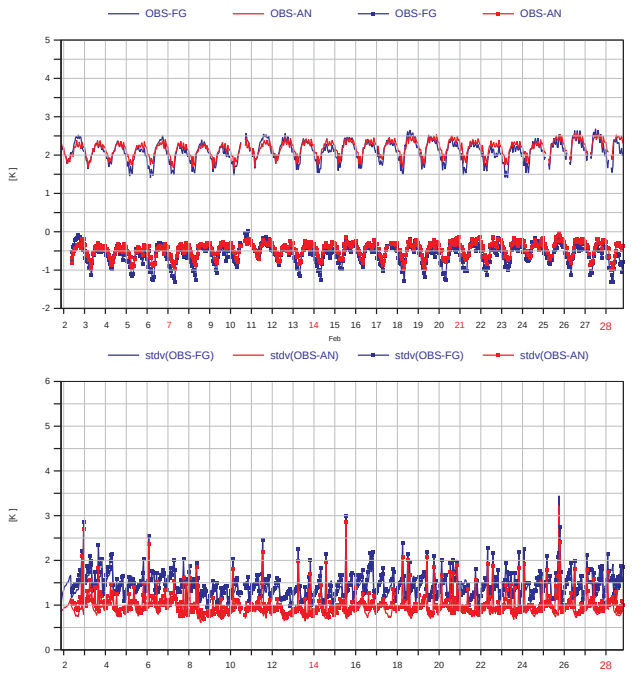

Figure 3: Time series of mean departure and standard deviation of GOES-12 (solid) and GOES-13 (solid with symbols) observed brightness temperature (in degrees K) minus corresponding model first guess (blue) and analysis (red) estimates for the WV-channel at 6.7μm over the period 2 to 28 February 2010.

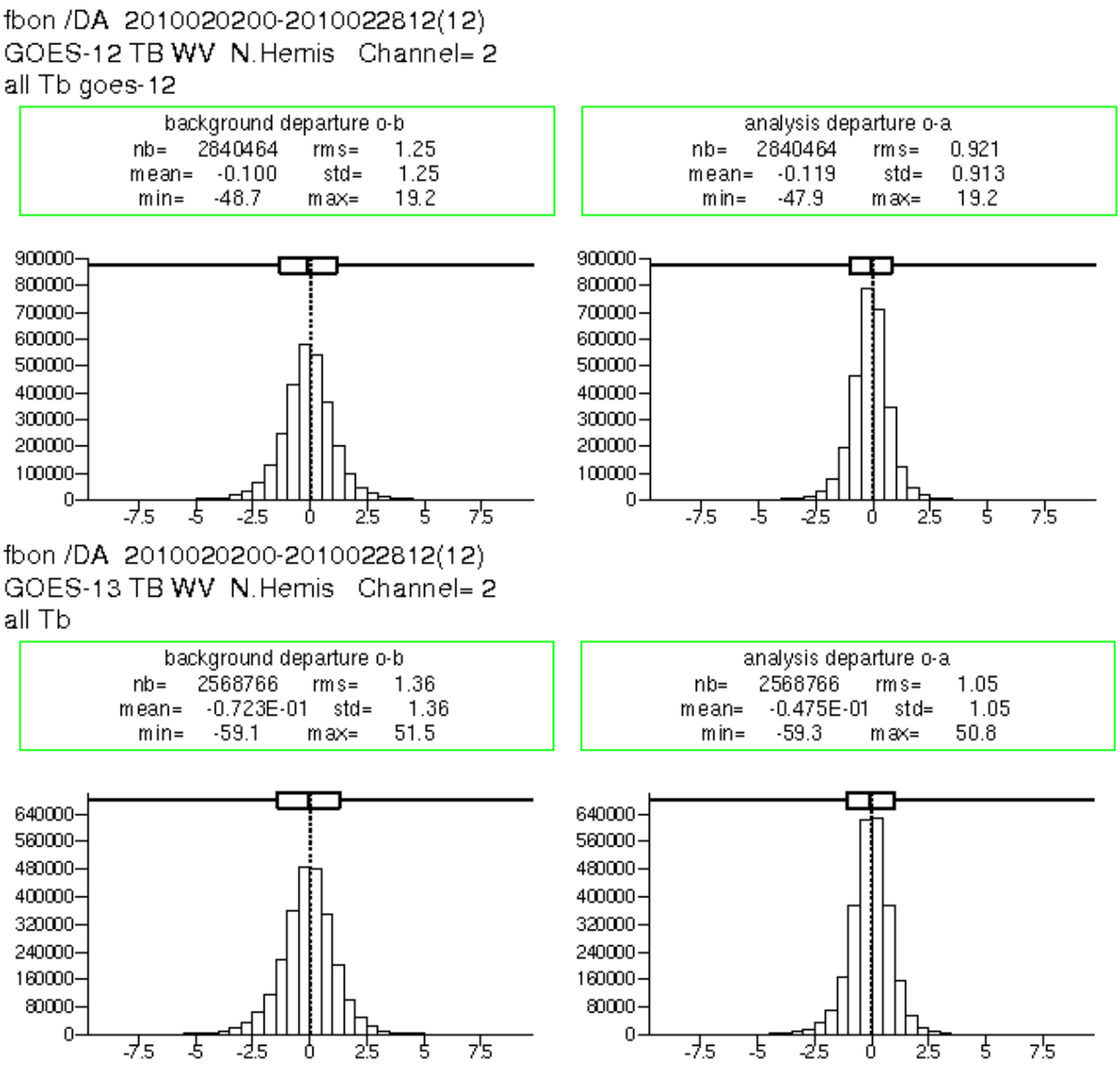

Figure 4: Standard deviation and mean of the first-guess and analysis departures calculated over the Northern Hemisphere for all WV-CSR from GOES-12 (top) and GOES-13 (bottom).

Also, an initial bias correction is carried out at this point by subtracting the bias estimate in the previous analysis from the calculated departure. The bias correction for geostationary water vapour radiances is based on a constant offset and a set of predictors (1000-300 hPa and 200-50 hPa layer thicknesses and total column water vapour).

In addition to the first guess checks and the variational quality control checks (Andersson and Järvinen, 1999) a few data selection criteria are specified in the blacklist. For example, CSR observations having satellite zenith angles larger than 60^o or being over high terrain (higher than 1.5km model orography) are excluded. We noted a negative bias (-0.5 K) for data around local midnight (*i.e.*, 5 UTC for GOES-13) and we excluded data during several hours in the night (*i.e.*, 1:30 UTC to 8:30 UTC). Also, data selection criteria are specified to discard cloud contaminated data. For example, in the WV channel data over land with smaller amounts of clear pixels in CSR mean (less than 70%) are excluded and also data over sea for which the model departure in the window channel is outside a chosen range [-3K, 3K]. Likewise, the observations in the window channel (IR at 10.7μm) are bias corrected. A thinning of geostationary CSR observations, yielding a spatial density of observations of about 125 km, is applied in operational practice before the assimilation. The observation error of GOES-13 CSR data is assumed uncorrelated and equal to 2 K.

In order to evaluate the impact of CSR from GOES-13 on the analysis and forecast two experiments have been performed with the ECMWF Integrated Forecasting System (cycle 36r2) at T511 (40 Km) resolution, 91 vertical levels and 12 hour 4D-Var for 1 to 28 April 2010:

- **Control** (experiment identifier *fdiu*): that used all conventional and satellite observations operationally assimilated except for clear-sky water vapour radiances from GOES-12 and GOES-13;
- **Experiment** (experiment identifier *fdiv*): clear-sky water vapour radiances from GOES-13 were assimilated in addition to the set of observations used in the **Control** experiment.

2.2.1 Analysis impact

Figure 5 shows the evolution of the background and analysis departures as well as the bias-corrected differences for the WV channel over the experiments period. When GOES-13 WV radiances are assimilated, the background fit has a mean standard deviation of about 1.11K, while the mean standard deviation of analysis fit is 0.68K.

The performance of these two experiments was also compared in terms of fit to other assimilated observations. Figures 6 and 7 show the standard deviation and the bias for the radiosonde east-west (u) component winds and relative humidity, respectively wich were used by the analysis in the Northern Hemisphere extratropics, Tropics and Southern hemisphere extratropics for the GOES-13 CSR assimilation experiment (*fdiv*-black) and the control (*fdiu*-red). The departures from the background field are shown with a solid line, while a dotted line is used for the departures from the analysis. The assimilation of GOES-13 CSR slightly improves the model fit to wind data from radiosondes over all areas. In the Tropics, the fit to radiosonde humidity observations is also improved as shown in figure 8. The biases are also displayed and they are similar or slightly improved comparatively to those of the control experiment.

2.2.2 Forecast impact

The impact of GOES-13 WV-CSR on forecast quality may be assessed in terms of normalized root mean square errors. Forecasts have been run from the analyses that assimilated GOES-13 CSR and from the control and each

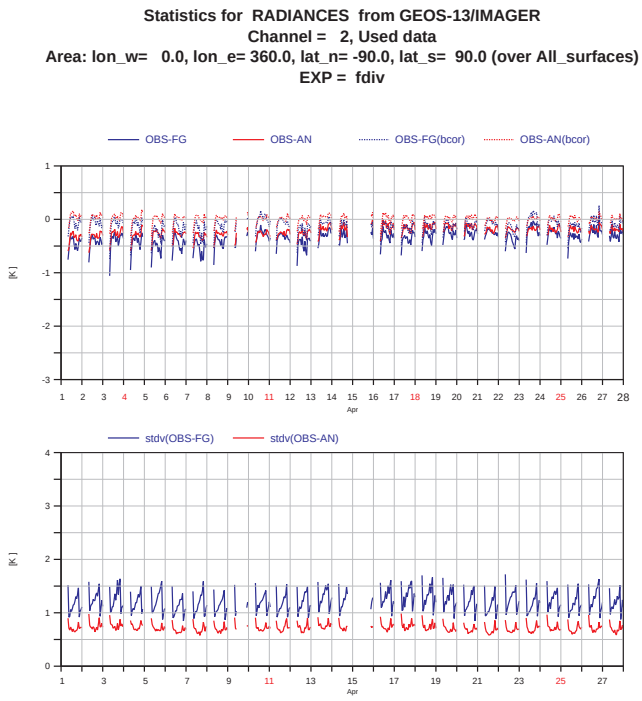

Figure 5: Time series of analysis and first-guess departure statistics for the active assimilation of GOES-13 WV-channel (6.7μm) for 1 to 28 April 2010.

verified versus the operational analysis over the 1-28 April 2010. Figure shows normalized RMS forecast error difference (experiment minus control divided by control) for 500 hPa height, relative humidity and vector wind in the Northern Hemisphere extratropics. A population of 26 forecasts was used to calculate the statistics (vertical error bars superimposed upon the plot indicate 95% confidence level for the null hypothesis that the RMS errors of the two experiments were identical). The impact of the GOES-13 CSR data is mainly neutral compared with the control experiment. The temperature, relative humidity and wind forecasts calculated at 300 hPa show also a neutral impact of GOES-13 over all the three regions (not shown).

3 Monitoring and assimilation experiments with MTSAT-2 CSR

Launched for the JMA on 18th February 2006, MTSAT-2 has been on standby in geostationary orbit at 145^o East until the 1st July 2010 when the operational use of the MTSAT-1R imaging function was switched over to that of MTSAT-2. Additionally, MTSAT-1R CSR and AMVs were swiched-over to MTSAT-2 from 00 UTC on 11th August 2010. We received at ECMWF pre-operational MTSAT-2 CSR since 00 UTC on 14th June 2010.

The specifications of the MTSAT-2 imager are the same as of MTSAT-1R JAMI. MTSAT-2 carries a 5-channel imager (one visible channel at 1 km resolution plus four IR channels at 4 km resolution at the sub-satellite point) and provides data coverage of the Western Pacific region. CSR are determinated hourly by taking the average of the brightness temperatures from the cloud-free pixels for each 16 x 16 pixel box (approximately 60 x 60 km^2 resolution at the sub-satellite point) and up to local zenith angles of 65^o .

At ECMWF, all the necessary modifications have been made to the IFS to support the monitoring and assimilation of CSR from MTSAT-2. The next section describes monitoring and assimilation experiments conducted

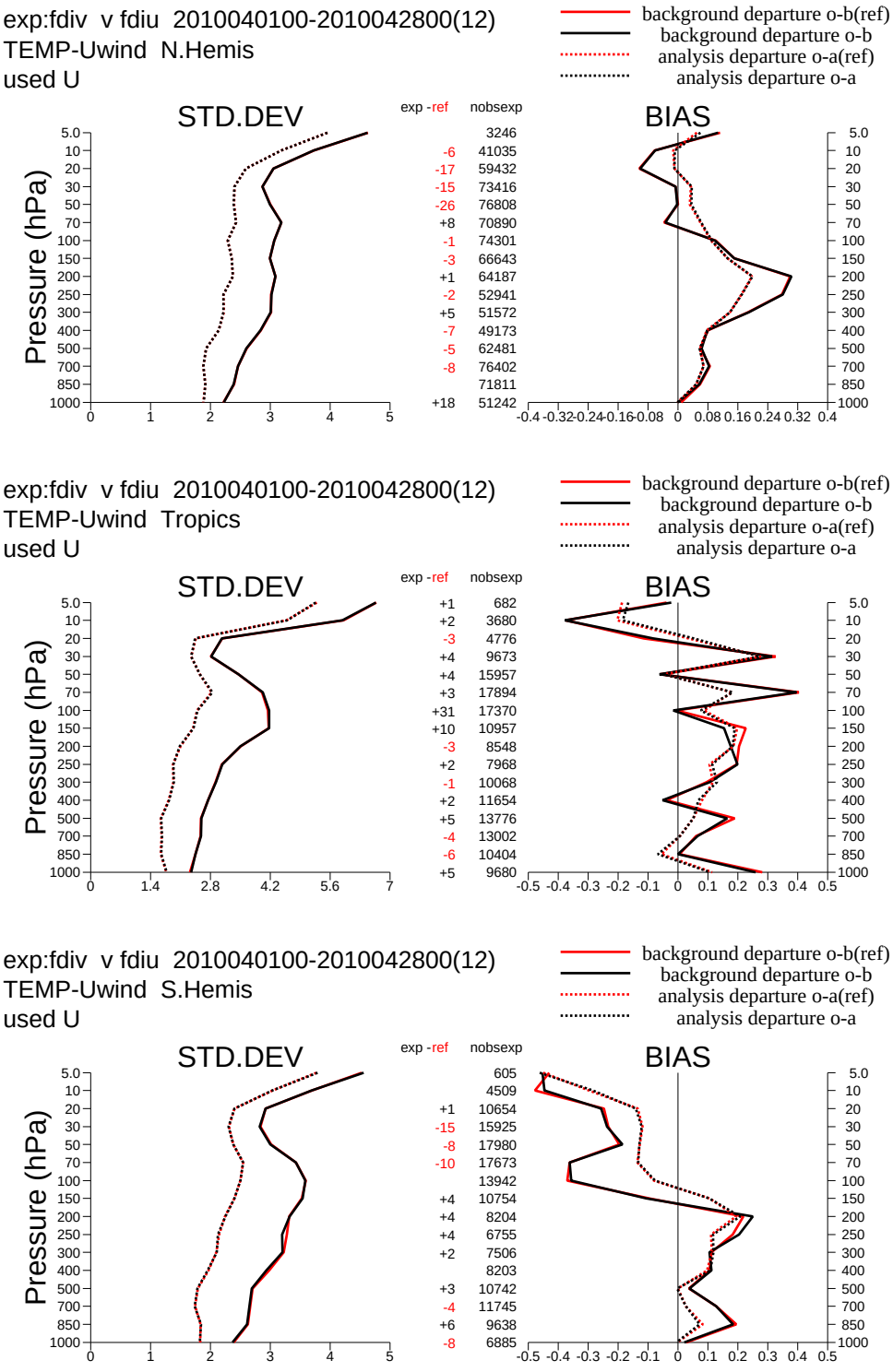

Figure 6: Standard deviation (left) and bias (right) for the departures of used radiosonde u-wind components in the Northern Hemisphere extratropics (top), Tropics (middle) and in the Southern Hemisphere extratropics (bottom) from the background (solid) and analysis (dotted) for the GOES-13 CSR assimilation experiment (fdiv-black) and the control (fdiu-red). "nobsexp" correspond to the number of observation assimilated in fdiv exp and the numbers in exp-ref correspond to the difference in number of observations between fdiv and fdiu experiments.

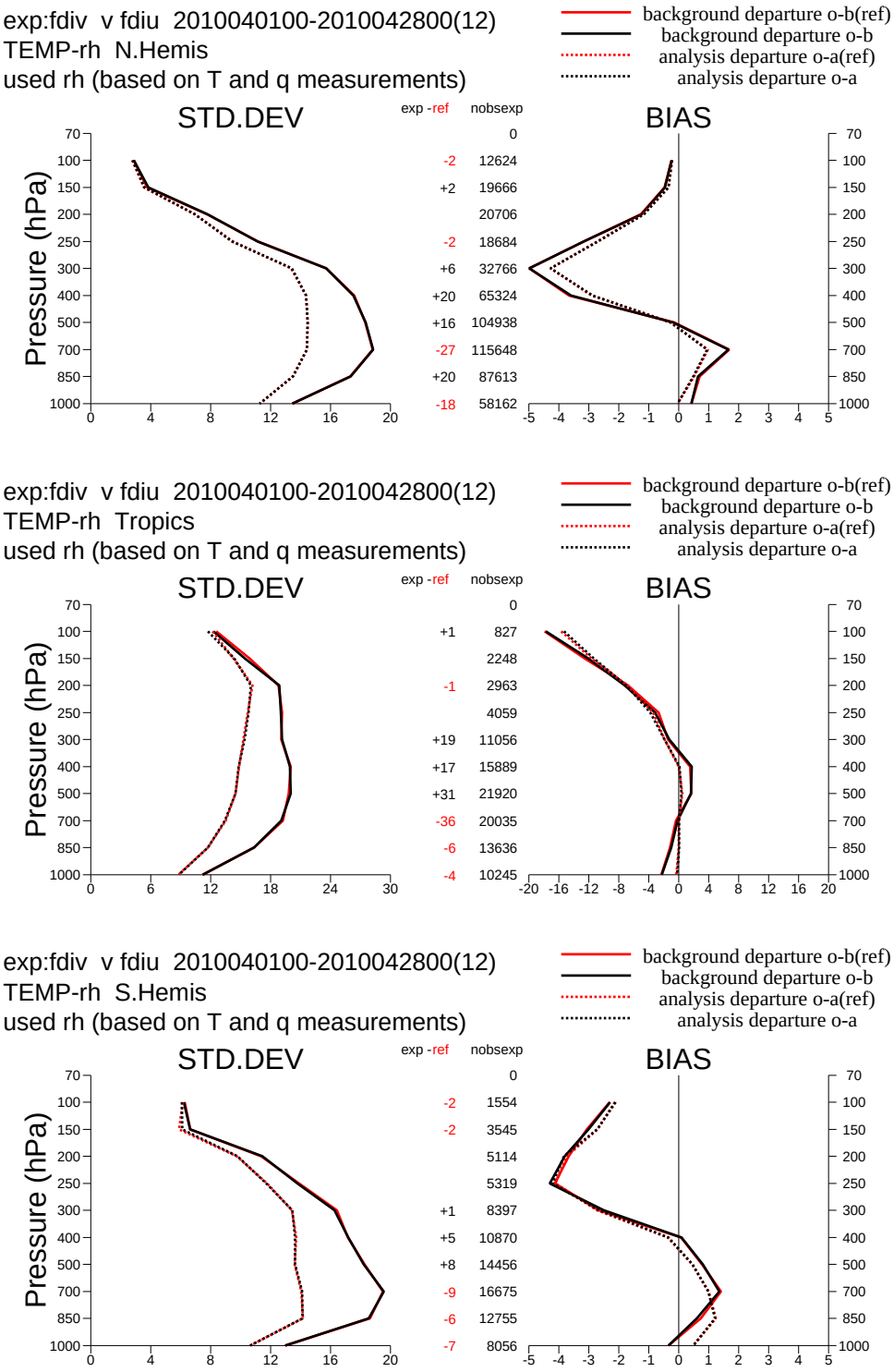

Figure 7: Same as figure 6 but the departures of used radiosonde relative humidity.

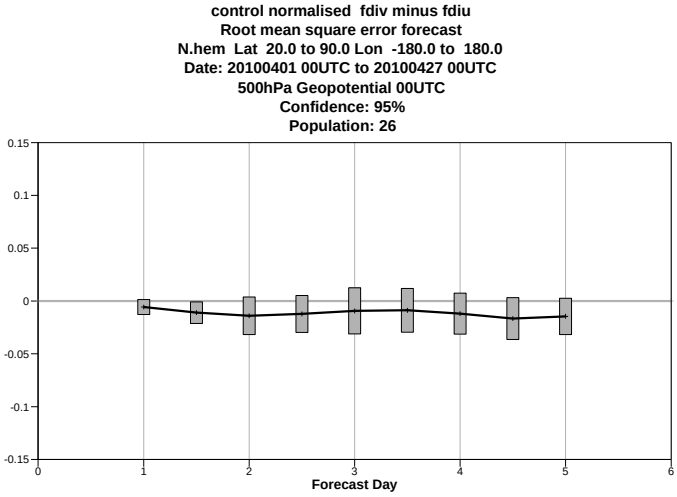

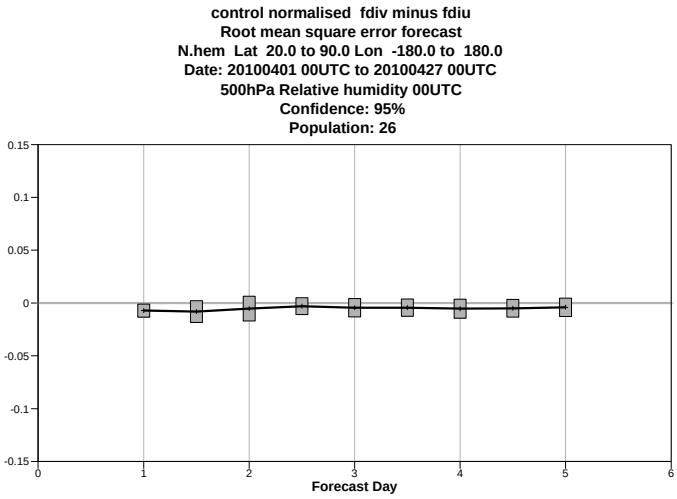

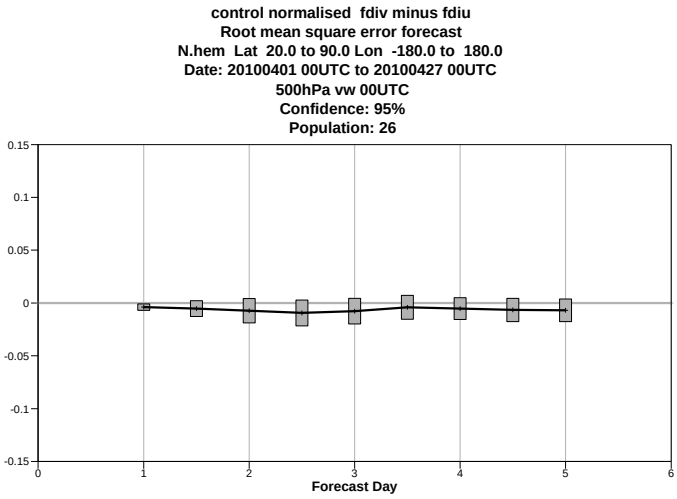

Figure 8: Normalized RMS forecast error difference (fdiv minus fdiu) divided by fdiu for 500 hPa geopotential height, relative humidity and vector wind in the Northern Hemisphere extratropics (20N-90N) evaluated over the 26 cases. Each system is verified versus the operational analysis.

off-line to asses the impact of pre-operational CSR from MTSAT-2 on analysis and forecast quality.

3.1 MTSAT-2 CSR: off-line monitoring experiments

The quality of the CSR from MTSAT-2 have been evaluated in the ECMWF system through the usual off-line passive monitoring experiments. All passive and active experiments are based on cycle 36r2 of ECMWF's 4D-Var data assimilation system similar to the operational configuration (Rabier et al., 2000). The study period was 16 June-15 July 2010 and we used a T511 horizontal resolution (40 km in grid point space) with a 91 vertical level configuration. 12-hourly incremental 4D-Var analyses were performed at T159 (125 km) and ten day forecasts were run from each 12 UTC analysis. The first experiment (experiment identifier *ff8d*) was designed to assimilate the operational set of observations (including CSR from MTSAT-1R) and to passively monitor CSR from MTSAT-2. Figures 9 and 10 show the time series (mean and standard deviation) of background and analysis departure statistics obtained over 1 month for the MTSAT-2 WV channel and for the window channel at 10.8μm, respectively. For the MTSAT-2 WV channel, the mean of the background and analysis departures after the bias correction is applied are -0.2K and -0.05K, respectively. The small value of the analysis departure is an indication that the analysis matches the observations very well. Standard deviations are respectively 1.4K and 0.8K for the background and analysis departures of MTSAT-2 WV-channel. Monitoring of the background departure CSR in the window channel showed a mean bias of -0.1K and a standard deviation of 1.06K.

There is a good consistency with values extracted from MTSAT-1R which was assimilated in this experiment. Figures 11 and 12 show the equivalent statistics for CSR from MTSAT-1 WV and window channels at 10.8μm, respectively. For the MTSAT-1 WV channel, the mean of the background and analysis departures after the bias correction is applied are -0.16K and -0.02K, respectively. Standard deviations are respectively 1.34K and 0.73K for the background and analysis departures. Monitoring in the window channel on MTSAT-1R with respect to the ECMWF model shows the channel to have a mean background departure of -0.5K and a standard deviation of background departure of about 1.06K.

Our second experiment (experiment identifier *ffih*) followed the same approach as the first experiment, except that CSR from MTSAT-1R were removed from the operational set of assimilated observations. Initial passive monitoring of the CSR from MTSAT-2 in this case followed the same steps as for the first experiment. As shown in figure 13, the WV channel showed an (O-B) bias of -0.25K and a standard deviation of (O-B) of about 1.49K. The mean and standard deviation of (O-A) are -0.10 and 0.96K, respectively. After the bias correction was applied, the bias corrected (O-B) and (O-A) are reduced to -0.2K and -0.05K. The mean (O-B) series for MTSAT-2 10.8μm channel shows a bias of -0.1K and a standard deviation of about 1.06K (see figure 14).

Passive monitoring of CSR data for the WV channel and window channel at 10.8μm of MTSAT-2 gave promising results. The next step was to proceed with assimilation experiments to assess the impact of MTSAT-2 water vapour radiance data on the assimilation and forecasting system..

3.2 MTSAT-2 CSR: 4D-Var assimilation results

The assimilation strategy of CSR from MTSAT-2 follow the one used for the assimilation of MTSAT-1R CSR (Peubey, 2007) and is summarized below:

- **Channel selection**: Only CSR from the WV channel are assimilated and data from the window channel (10.8μm) are used for quality control.

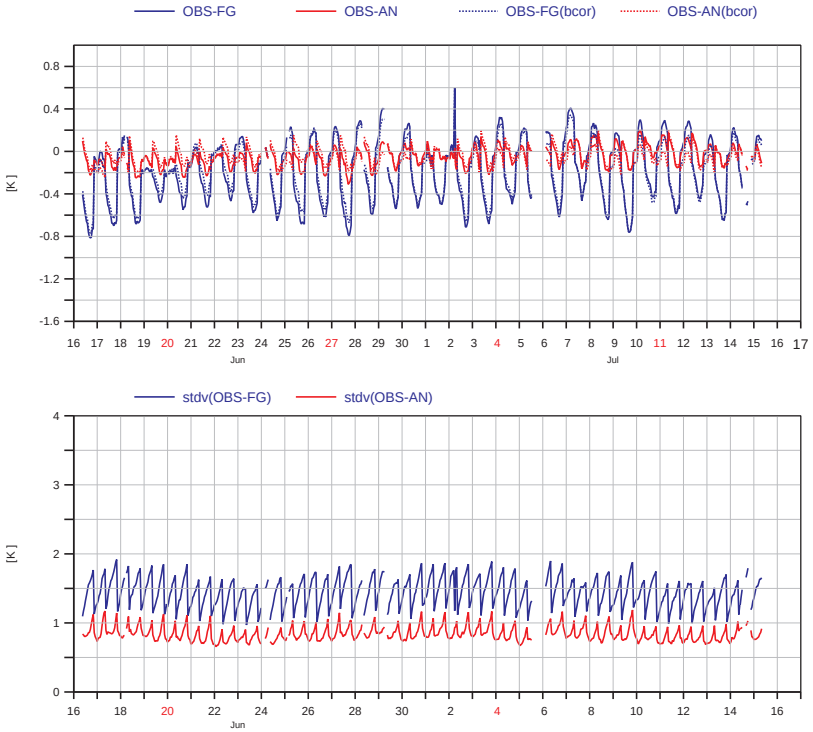

Figure 9: Time series of first-guess and analysis departure statistics, in K, for the off-line passive monitoring of MTSAT-2 WV-channel (6.8μm) over the period 16 June to 15 July 2010.

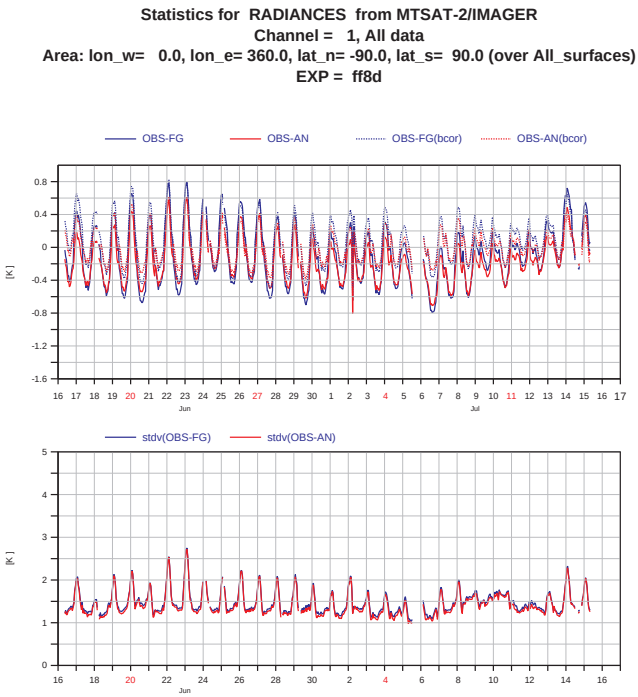

Figure 10: Time series of first-guess and analysis departure statistics, in K, for the off-line passive monitoring of MTSAT-2 window channel (10.8μm) over the period 16 June to 15 July 2010.

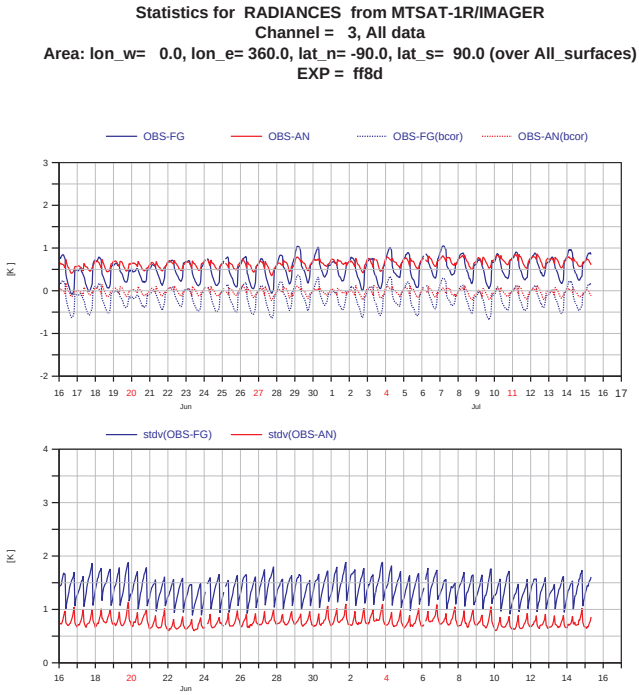

Figure 11: Time series of first-guess and analysis departure statistics, in K, for MTSAT-1R WV-channel (6.8µm) over the period 16 June to 15 July 2010.

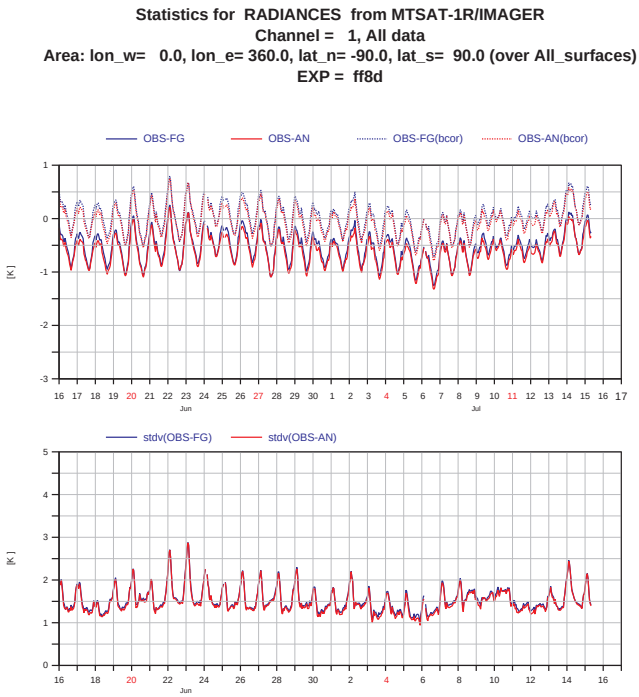

Figure 12: Time series of analysis first-guess and analysis departure statistics, in K, for MTSAT-1R window-channel (10.8µm) over the period 16 June to 15 July 2010.

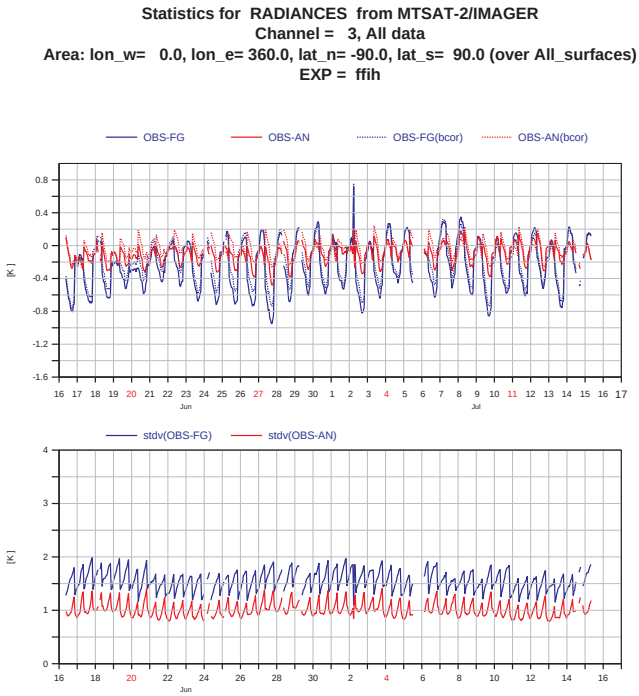

Figure 13: As Fig.9 but for the experiment ffih where CSR from MTSAT-1R were removed from the operational set of assimilated observations.

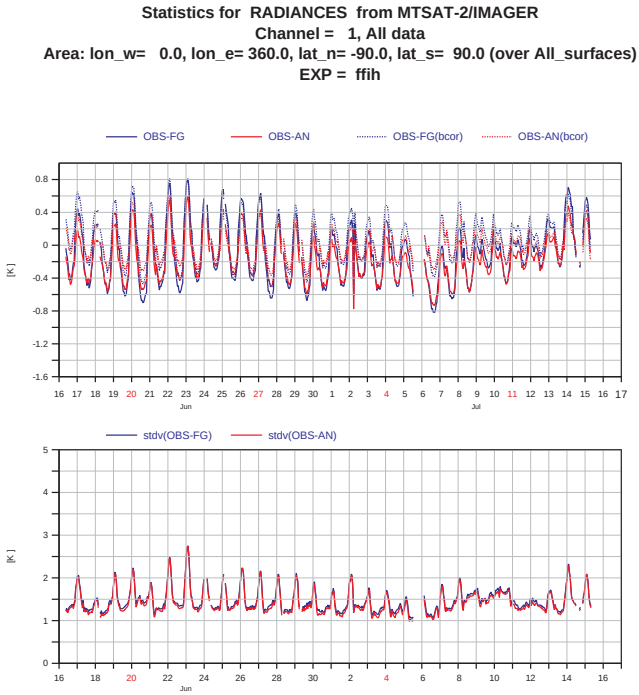

Figure 14: As Fig.10 but for the experiment ffih where CSR from MTSAT-1R were removed from the operational set of assimilated observations.

- **Bias correction**: Both experiments use variational bias correction (Dee 2004). The bias correction for geostationary water vapour radiances is based on a constant offset and a set of predictors (1000-300 hPa and 200-50 hPa layer thicknesses and total column water vapour).
- **Quality control**: In the WV channel, two criteria are used to reject CSR: a) all CSR from MTSAT-2 having the percentage of clear pixels less than 50% are rejected; b) over sea, data having a model departure in the window channel outside the $\pm$3K are rejected.
  In the window channel, which have contributions from the surface, CSR over land or having a percentage of clear pixels less than 70% are rejected.
- **Blacklist**: CSR from MTSAT-2 with scanning angle greater than 60^o or above high orography (1.5km) were excluded.
- **Observation error**: CSR from MTSAT-2 are assumed uncorrelated and a constant value of 2K has been assigned to the error standard deviation.

In order to evaluate the impact of CSR from MTSAT-2 on the analysis and forecast two experiments have been performed:

- **Control** (experiment identifier *ff8i*): that used all conventional and satellite observations operationally assimilated in cycle 36r2 except for clear-sky water vapour radiances from MTSAT-1R and MTSAT-2;
- **Experiment** (experiment identifier *ff8e*): clear-sky water vapour radiances from MTSAT-2 were assimilated in addition to the set of observations used in the **Control** experiment.

3.2.1 Analysis impact

Figure 15 shows the evolution of the background and analysis departures as well as the bias corrected differences for the assimilated MTSAT-2 CSR in the WV channel over the experiment period. When MTSAT-2 WV radiances are assimilated, the standard deviation of (O-B) varies around 1.33K and the mean of the background departure are reduced to -0.16K after the bias correction. Note that, the mean and standard deviation of (O-A) are -0.01 and 0.71K, respectively.

When comparing the **Experiment** (*ff8e*) and the **Control** (*ff8i*) in terms of fit to other assimilated observations, there is a small change in the departure statistics of the radiosonde temperature, relative humidity and wind observations. Figs. 16 and 17 show that the assimilation of MTSAT-2 CSR slightly improves the model fit to radiosonde v-wind data over the Northern Hemisphere extratropics as well as the model fit to radiosonde relative humidity over the Tropics.

Other differences in the standard deviation can be reported for the AMSU-B/MHS humidity sounding channels. As seen in Figs. 18 and 19 the assimilation of WV CSR from MTSAT-2 reduces the standard deviation of the model first-guess departures of other datasets, as for AMSU-B and MHS.

3.2.2 Forecast impact

We have investigated the forecast scores for geopotential, temperature, wind, and relative humidity at differents tropospheric levels where MTSAT-2 imager have their largest impact. As a summary of the impacts, the geopotential and relative humidity forecast scores at 500 hPa are presented in Figs. 20 and 21. Both figures show the normalised difference in RMS error between **Experiment** and **Control** as a function of forecast time

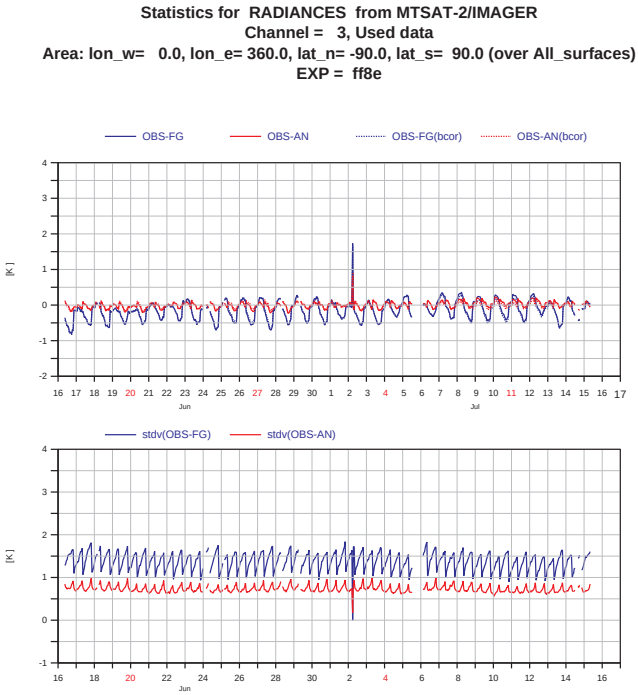

Figure 15: Time series of first-guess and analysis departure statistics, in K, for the off-line active assimilation of MTSAT-2 WV-channel (6.8µm) for the period 16 June to 15 July 2010.

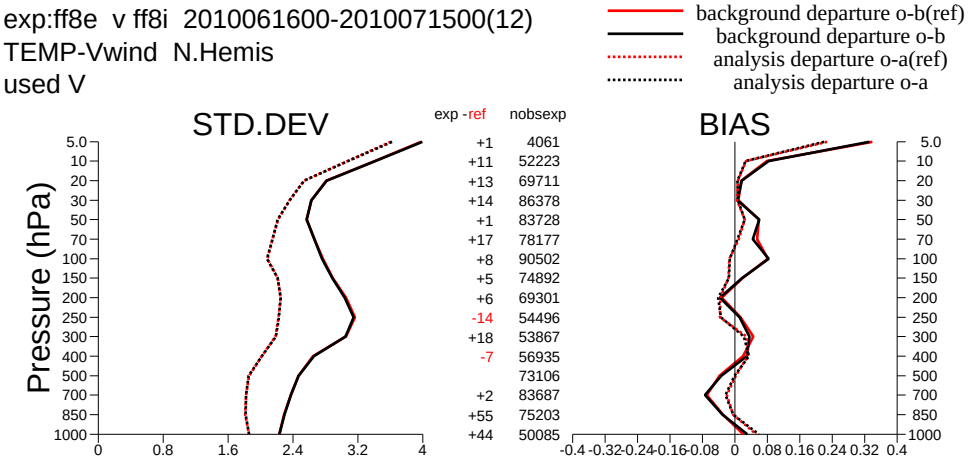

Figure 16: Standard deviations (left panel) and means (right panel), in K, for the departures of used radiosonde v-wind components in the Northern Hemisphere extratropics from the background (solid) and analysis (dotted) for the MTSAT-2 CSR assimilation experiment (ff8e-black) and the control (ff8i-red).The number of used observations are displayed between the two plots, with the difference relative to the Control shown in the column exp-ref.

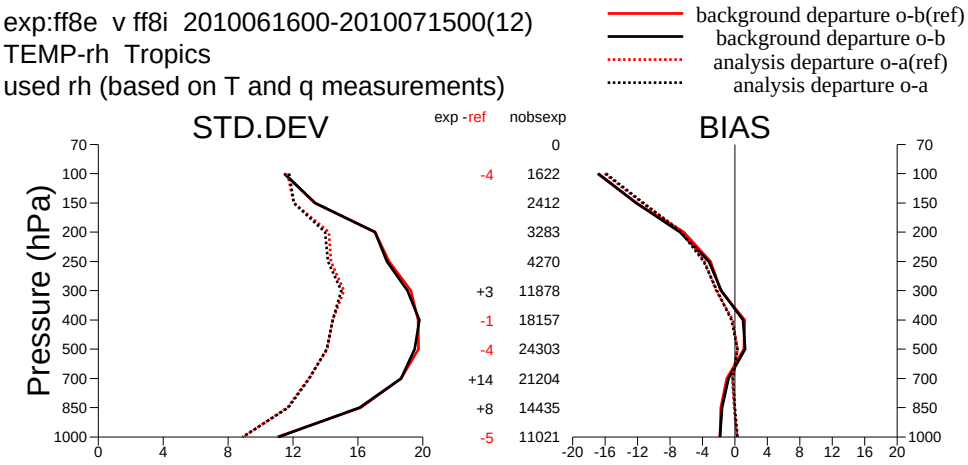

Figure 17: As Fig. 16 but the departures of used radiosonde relative humidity over the Tropics for the period 16 June to 15 July 2010.

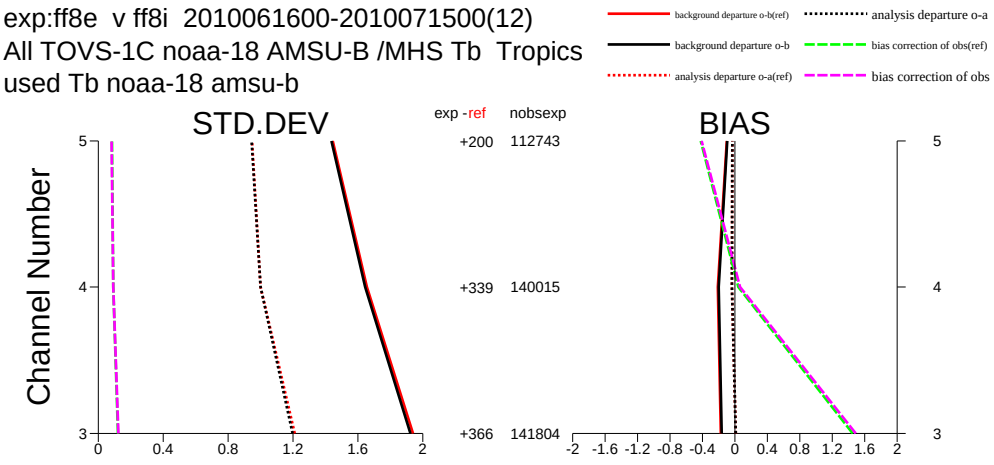

Figure 18: Standard deviations (left panel) and means (right panel), in K, for background departures (solid lines), analysis departures (dotted lines), and bias corrections (dashed lines) for used NOAA-18 AMSU-B radiances over the Tropics for the period 16 June to 15 July 2010. Statistics for the MTSAT-2 CSR assimilation experiment are shown in black and magenta, whereas statistics for the Control are shown in red and green. The number of used observations are displayed between the two plots, with the difference relative to the Control shown in the column exp-ref.

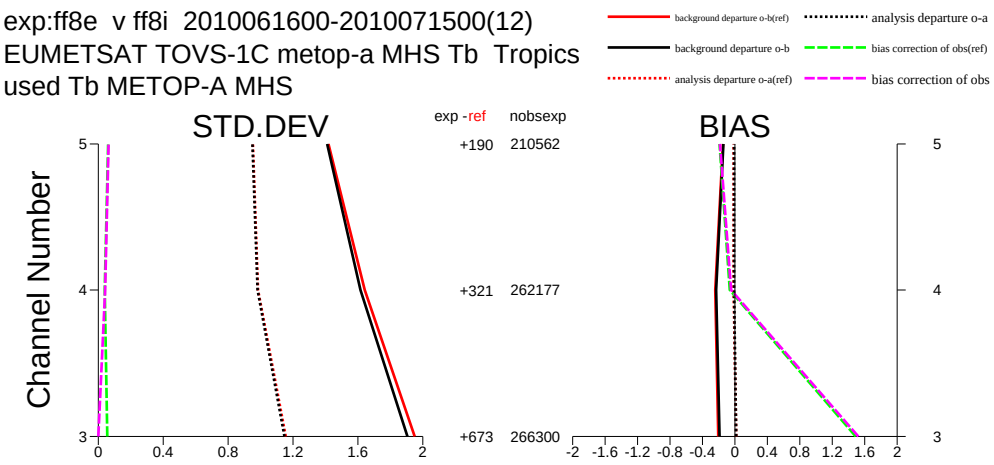

Figure 19: As Fig. 18 but for used MetOp-A MHS radiances over the Tropics for the period 16 June to 15 July 2010.

in days. Negative values indicate that **Experiment** has smaller errors than **Control** and hence represents an improvement compared to **Control**. Error bars indicate confidence intervals at the 95% level. Both experiments have been verified against the operational ECMWF analysis. Figs. 20 and 21 suggest that forecast scores for geopotential and relative humidity at 500 hPa are, in general, not statistically significantly different for the experiment that assimilated WV CSR from MTSAT-2 and the control.

4 Progress towards the assimilation of geostationary all sky radiances (ASR)

Work to exploit cloud-affected geostationary radiances from the Meteosat-9 satellite into ECMWF four dimensional variational assimilation (4D-Var) is well under way. In 2009 EUMETSAT has started to disseminate a new all-sky radiance (ASR) product from Meteosat-9 SEVIRI observations. The ASR product contains information on mean brightness temperatures for both clear and cloudy regions, thereby extending the information already available in the CSR product, which is also included in the ASR.

The overcast cloudy scheme proposed by McNally (2009) and used operationally at ECMWF to directly assimilate cloud-affected infrared radiances from AIRS/IASI and HIRS polar orbiter data was extended to make use of the all-sky radiance products produced by EUMETSAT from Meteosat-9 SEVIRI data. The key elements of the cloudy scheme and the difficulties inherent to cloud-affected data assimilation was presented by McNally (2009). In this study, the approach introduced by Eyre and Menzel (1989) has been used to retrieve values of cloud parameters (cloud top pressure and effective cloud fraction, as initial estimates) which maximize the sum of the squared differences between observations and simulated cloudy radiances. This method uses a simplistic cloud model (single layer of opaque or semitransparent thin cloud with a homogeneous emissivity) to compute cloudy radiances. For Meteosat-9, observed radiances in channels 6 (10.8μm) and 8 (13.4μm) are used in the estimation pf cloud parameters. Cloud cover and height are diagnosed from the data and in overcast scenes, cloud parameters are adjusted simultaneously with atmospheric temperature and humidity during the 4D-Var.

Our first experiment is an ASR addition onto a no-satellite baseline experiment over a one-month period from 10 February to 10 March 2010. The baseline is initialized from the ECMWF operational analysis on 2 February

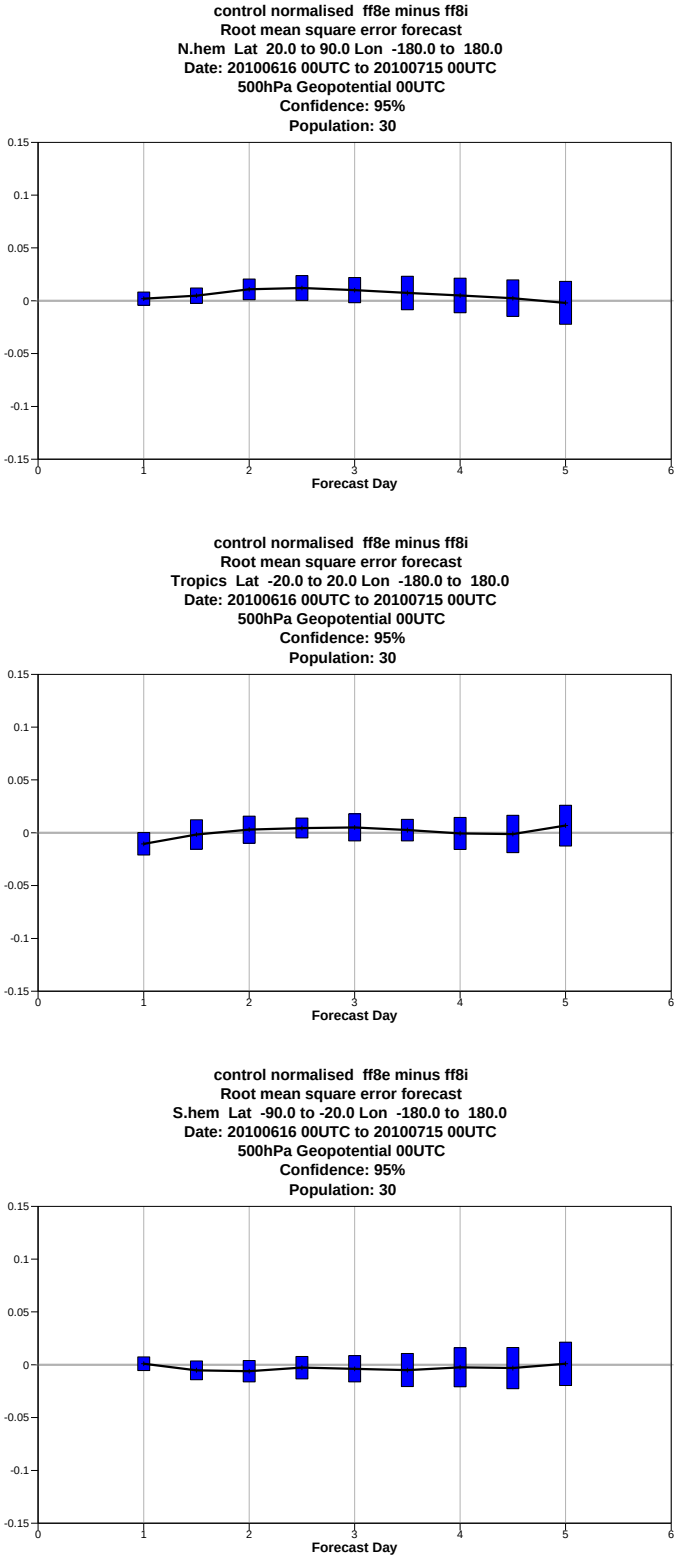

Figure 20: Normalised differences in the root mean square forecast error between the Experiment (ff8e) and the Control (ff8i) against forecast time in days for the 500 hPa geopotential over Northern Hemisphere extratropics (top), Tropics (middle) and Southern Hemisphere extratropics (bottom). Both experiments have been verified against the operational ECMWF analysis. Negative values indicate a reduction in forecast error for the Experiment. Error bar indicate confidence intervals at the 95% confidence level.

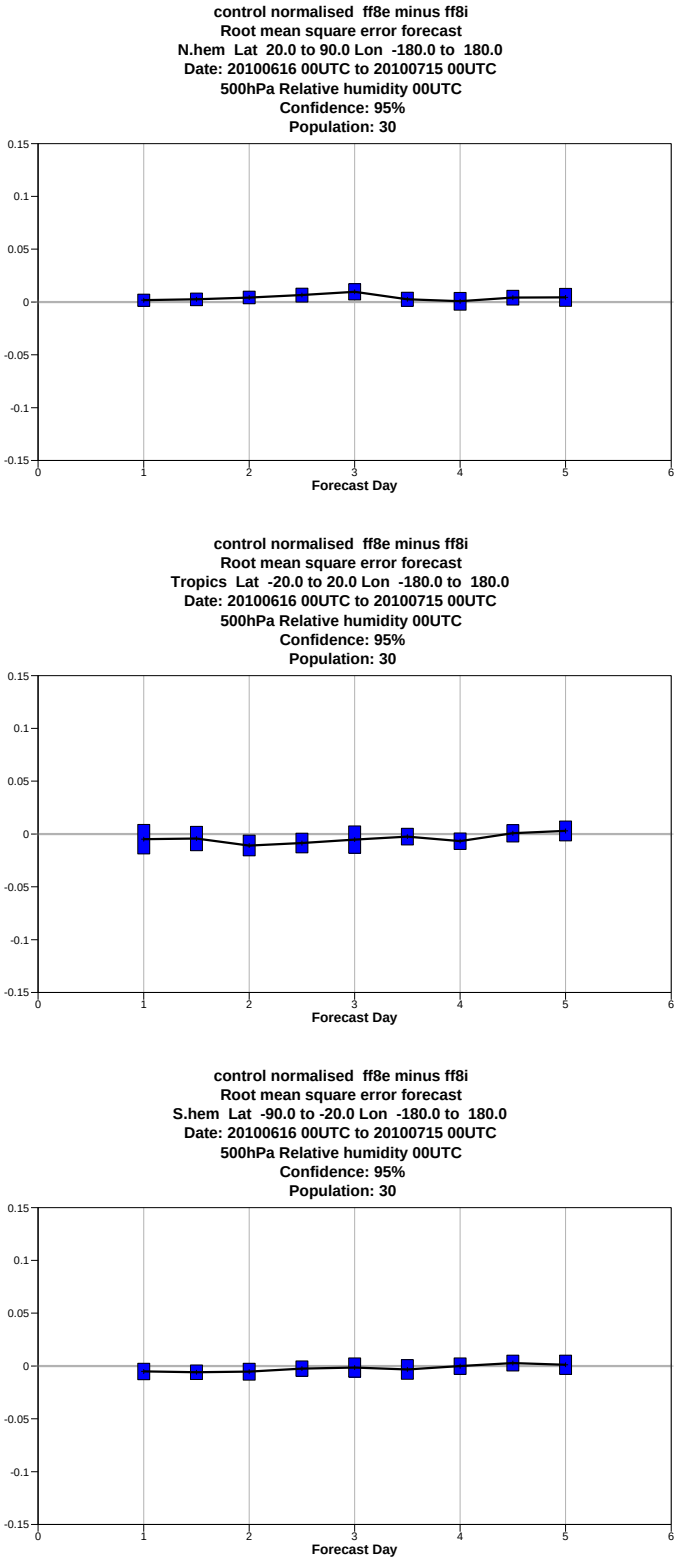

Figure 21: As Fig. 20 but for 500 hPa relative humidity.

2010 and runs at a lower T511 spatial resolution. The only assimilated observations in the baseline experiment are conventional data from radiosondes, aircraft and surface observations. The ASR experiment, started from a degraded baseline experiment over a period of 8 days, makes additional use of overcast (estimated cloud fraction equal 1) SEVIRI observations from Meteosat-9. However, prior to the assimilation, overcast scenes over land or with cloud top below 900 hPa are excluded (McNally, 2009).

We first compared the effective cloud fraction estimated from the observation with the independent estimates produced and provided by EUMETSAT. Figure 22 shown an example of cloud fraction for the first 12-hours analysis cycle for high (100-300hPa), middle (300-600hPa) and low (600-900hPa) clouds. Our estimation of cloud fraction agrees well with EUMETSATs independent estimation especially for the overcast scenes.

The differences between temperature, humidity and wind analysis increments in the ASR overcast experiment and baseline has been examinated for the first 12-h analysis cycle (0000 UTC on 09 February 2010). The increment differences are shown in Figure 23 for temperature (left side) and humidity and winds (right side) at three different levels: 300hPa (top), 500hPa (middle) and 850hPa (bottom). The assimilation of overcast geostationary radiances affects temperatures, humidity and winds in areas where overcast radiance observation are available. Figure 24 shows the differences between the ASR overcast and baseline experiments in terms of the RMS temperature, humidity and wind analysis increments, calculated over one month at the same levels as in Figure 23. The changes due to the use of overcast data spread by advection into other areas after many successive cycles.

Recent study by Peubey and McNally (2009) investigated the impact of geostationary clear-sky radiances and atmospheric motion vectors derived from geostationary satellites on 4D-Var wind analyses. The most important mechanism through which the assimilation of CSR can impact wind analysis is the humidity tracer advection. The main objective of this study is to extend the humidity tracing capability, previously demonstrated only in clear sky, to cloudy regions, to obtain an all-sky constraint the atmospheric wind field with geostationary radiances.

The objective for the coming months is to work on assimilation of Meteosat-9 overcast cloudy data in addition to the WV clear-sky radiances from the two water-vapour channels currently operational assimilated. The extra cloudy data retained should cover the areas where clear sky radiances are not available. As part of this work, we will quantify the impact of the new data set (CSR+overcast) on the wind analysis and compare with AMVs impact. It is hoped that this analysis will help to understand some of the issues associated with AMVs in terms of bias and error characterization as well as the underlying assumption that the motion of the tracked features can help to characterize the atmospheric wind field.

5 Discussion and conclusions

This report has described passive monitoring and active assimilation experiments, done in order to operationally assimilate WV-CSR from GOES-13 and MTSAT-2 alongside WV-CSR from other geostationary satellites (Peubey and McNally, 2009; Munro *et al.*, 2004; Köpken *et al.*, 2004).

Monitoring experiments have shown that the quality of the data from the replacement satellites was stable and comparable with those of their predecessors, aiding a smooth transition to the operational use of the new data sets. At ECMWF WV CSR from GOES-13 are assimilated operationally since 29 April 2010. MTSAT-2 CSR were discontinued from October 7, 2010 due to failure of image data processing on the MTSAT-2 ground system. On 13th October 2010 JMA decided to continue the backup observation by MTSAT-1R until 03 UTC on 22 December 2010. As a result, JMA continued to disseminate MTSAT-1R CSR until the end of the backup observation by MTSAT-1R. In these conditions, we decided to delay the operational as-

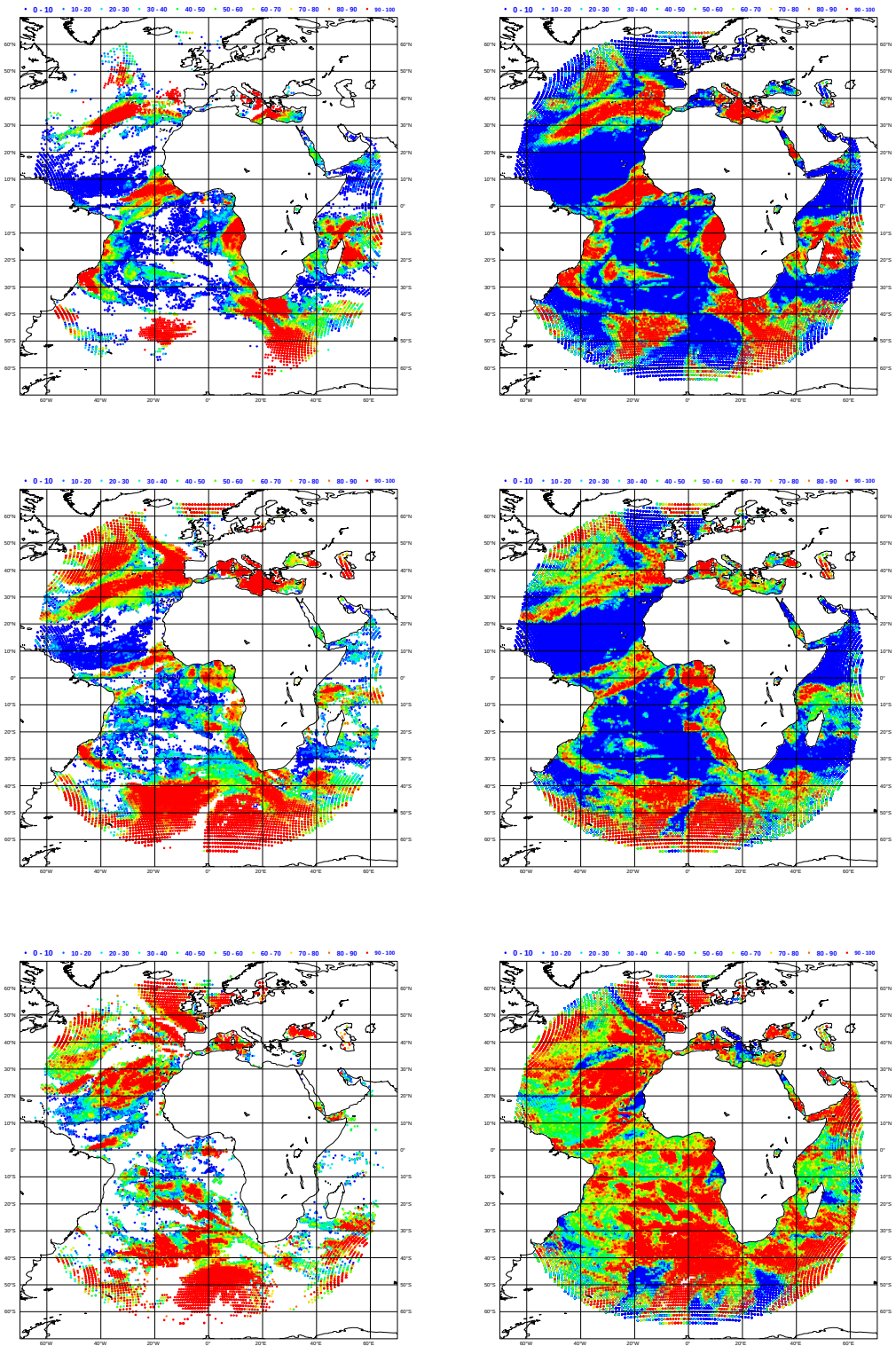

Figure 22: The cloud fraction obtained using Eyre and Menzel (1989) approach (left) and provided within the ASR file produced by EUMETSAT (right). The cloud top pressure is between 100 and 300 hPa (top), 300 and 600 hPa (niddle) and 600 and 900 hPa (bottom).

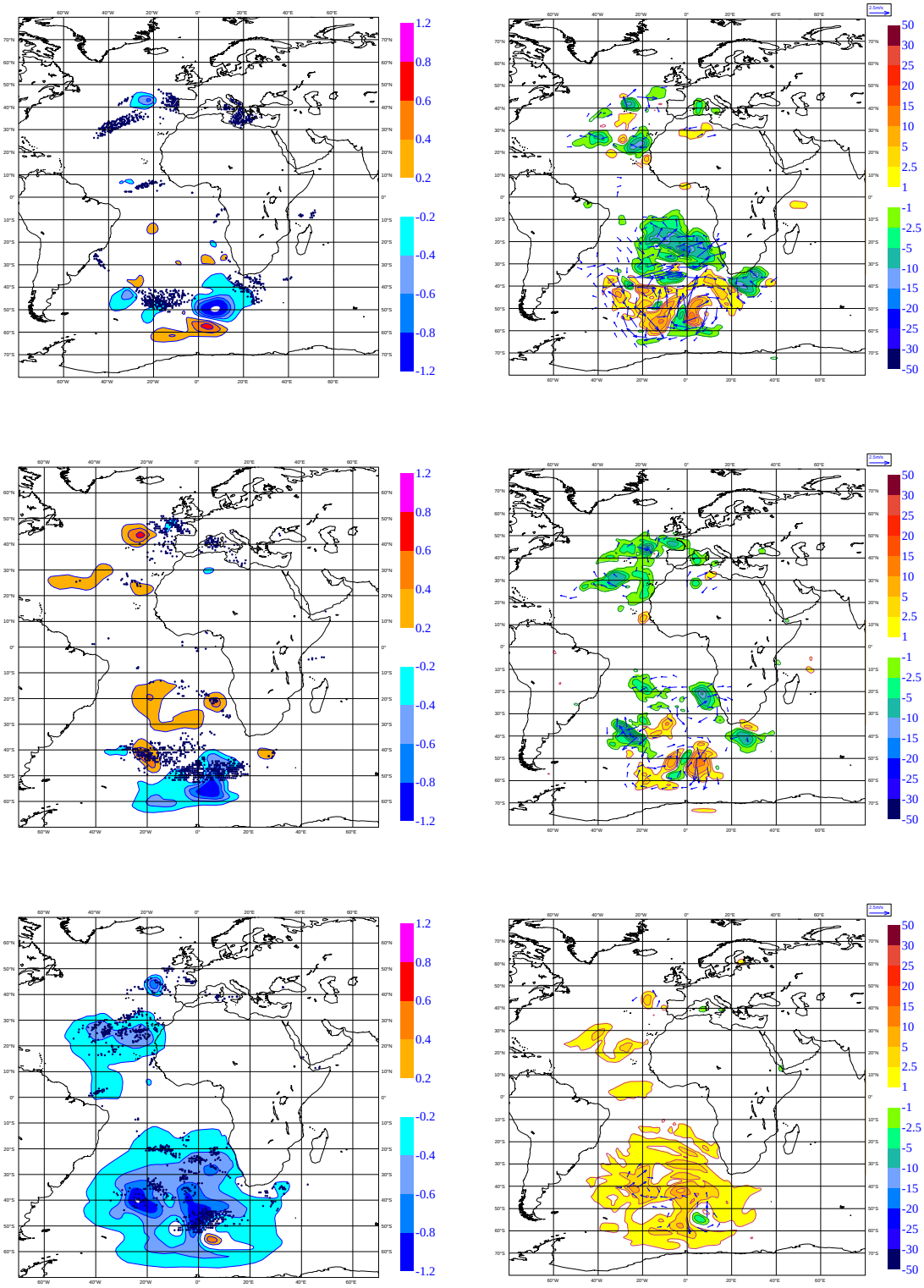

Figure 23: For the first 12-hour analysis cycle (0000 UTC on 09 February 2010), the increments in temperature (in K on the left), relative humidity (as a percentage) and winds (m/s, on the right side) produced by the ASRs (no-satellite context) (top) 300 hPa, (middle) 500 hPa and (bottom) 850 hPa. The black dots shows the location of overcast scenes with cloud height between (top) 400-200 K hPa , (middle) 750-400 hPa and (bottom) 900-750 hPa.

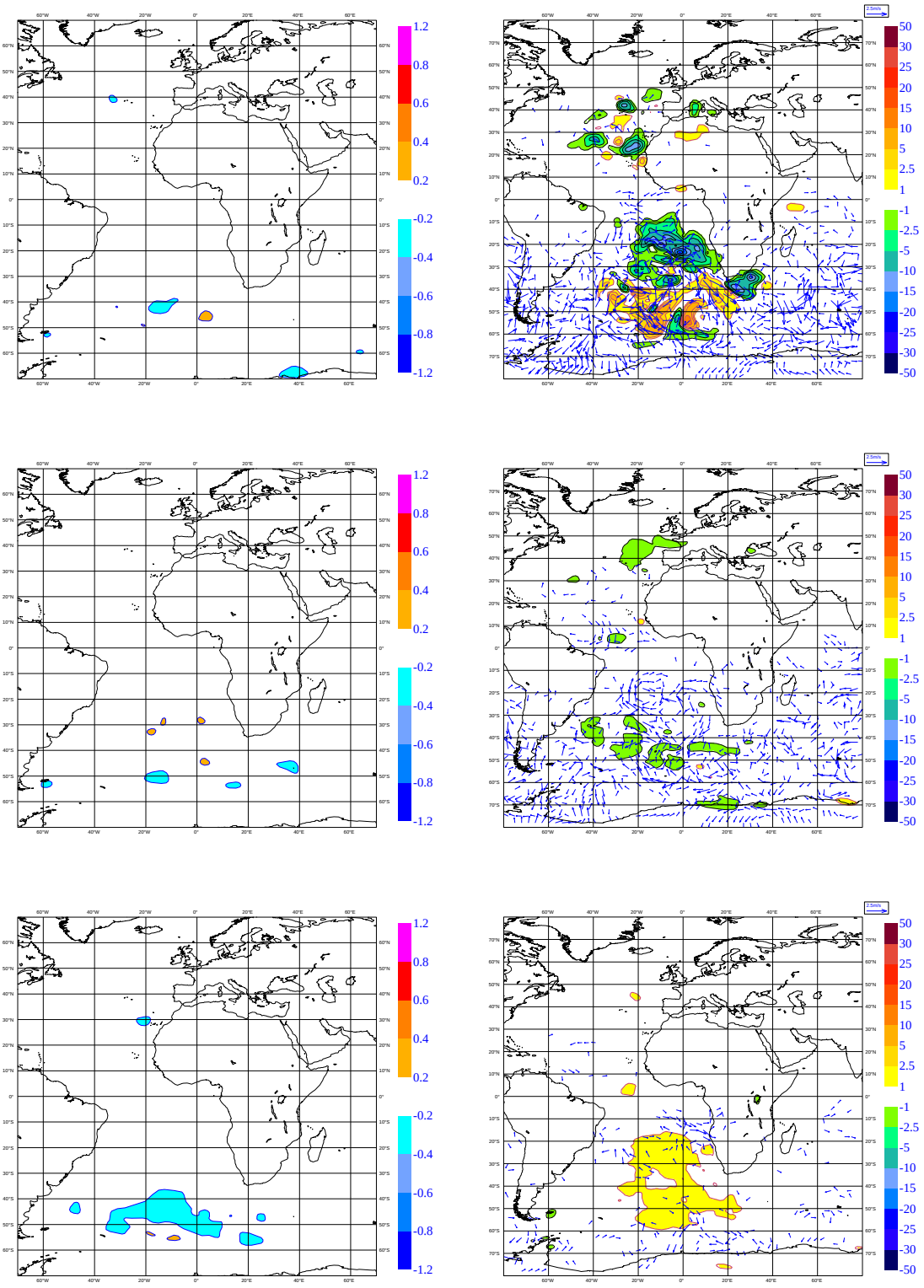

Figure 24: RMS temperature (left), relative humidity and winds (right) increment differences (EXPT minus CTRL) at (top) 300 hPa, (middle) 500 hPa and (bottom) 850 hPa averaged over one month period (10 February to 10 March 2010).

similation of MTSAT-2 WV CSR in ECMWF 4D-Var system until January 2011 when MTSAT-2 was back to operational. We started to operationally assimilating MTSAT-2 WV CSR in ECMWF 4D-Var system in cycle 36r4 on 25 January 2011. Monitoring statistics of geostationary CSR including time-averaged mean fields, time series of area averages and Hovmöller zonal mean fields of geostationary CSR data can be found at http://www.ecmwf.int/products/forecasts/d/charts/monitoring/satellite/geos. The assimilation results of water vapour CSR from GOES-13 and MTSAT-2 does not appear to substantially change diagnostics from the analyses and the impact on the 1 to 5 day forecasts appears to be generally neutral.

Work to exploit all-sky radiance (ASR) product from Meteosat-9 SEVIRI observations is well under way. Preliminary studies show that the initial cloud parameters derived from the ASR SEVIRI observations agree very well with EUMETSAT's independent evaluation of the cloud conditions. Assimilation experiments with overcast radiances affects temperatures, humidity and winds increments in areas where overcast radiance observation are available. The next step will be to perform experiments with Meteosat-9 overcast cloudy data assimilated in addition to the clear-sky radiances from the two water-vapour channels. The impact of all-sky geostationary radiances on wind analyses will be further investigated and results on quantifying the impact of the ASR on the wind analysis will be presented and compared with the impact of clear-sky radiances and AMVs.

6 Acknowledgements

The authors would like to thank a large group of people at ECMWF for help with this work: Carole Peubey, Peter Bauer, Niels Bormann, Alan Geer and Jean-Noël Thépaut for helpfull discussions and feedback, Mohamed Dahoui for help with observation statistics, Anne Fouilloux for help with ODB aspects of the work, Ioannis Mallas and Milan Dragosavac for assistance with BUFR encoding and Jan Haseler for advice and support on the data assimilation experiments. Cristina Lupu is funded by the EUMETSAT Fellowship Programme.

References

Andersson, E. and H. Järvinen, 1999: Variational quality control. *Q. J. R. Meteorol. Soc.* **125**, 697-722.

Dee, D. P., 2004: Variational bias correction of radiance data in the ECMWF system. Proceedings of the ECMWF workshop on assimilation of high spectral resolution sounders in NWP, 28 June-1 July 2004. Reading, UK.

Eyre, J. R. and W. P. Menzel, 1989: Retrieval of cloud parameters from satellite sounder data: A simulation study. *J. Appl. Meteor.*, **28**, 267275.

Köpken, C., G. Kelly and J-N. Thépaut, 2004: Assimilation of Meteosat radiance data within the 4D-Var system at ECMWF: Data quality monitoring, bias correction and single-cycle experiments. *Q. J. R. Meteorol. Soc.* **130**, 2293-2313G.

Lupu, C., 2010: Assimilation of GOES-13 Clear Sky Radiances. Research Departament Memorandum, R43.8 / CL/ 1046, 18pp.

Lupu, C., 2010: Monitoring and assimilation experiments with MTSAT-2 clear-sky radiances. Research Departament Memorandum, R43.8/CL/10108, 13pp.

McNally, A., 2009: The direct assimilation of cloud-affected satellite infrared radiances in the ECMWF 4D-Var. *Q. J. R. Meteorol. Soc.* **135**, 1214-1229.

Munro, R., C. Köpken, G. Kelly, J-N. Thépaut and R. Saunders, 2004: Assimilation of Meteosat radiance data within the 4D-Var system at ECMWF: Assimilation experiments and forecast impact. *Q. J. R. Meteorol. Soc.* **130**, 2277-2292.

Peubey, C., 2007: Assimilation of MTSAT Clear Sky Radiances. Research Departament Memorandum, R43.8/CP/0801, 14pp.

Peubey, C., and A. P. McNally, 2009: Characterization of the impact of geostationary clear sky radiances on wind analyses in a 4D-Var context. *Q. J. R. Meteorol. Soc.* **135**, 1863-1876.

Rabier, F., H. Järvinen, E. Klinker, J.-F. Mahfouf, and A. Simmons, 2000: The ECMWF operational implementation of four-dimensional variational assimilation. I: Experimental results with simplified physics.*Q. J. R. Meteorol. Soc.* **126**, 1148-1170.

Salmond, D. *et al.*, 2010: IFS Memorandum Cycle CY36R3. Research Departament Memorandum, R48.3 / DS / 1022, 34pp.

APPENDIX: Accronyms and abbreviations

4D-Var	Four-dimensional variational data assimilation
AIRS	Atmospheric InfraRed Sounder
AMVs	Atmospheric Motion Vectors
CIMSS	Cooperative Institute for Meteorological Satellite Studies
CSR	Clear Sky Radiances
ASR	All Sky Radiances
ECMWF	European Centre for Medium Range Weather Forecast
EUMETSAT	European Organisation for the Exploitation of Meteorological Satellites
GOES	Geostationary Operational Environmental Satellite
HIRS	High Resolution Infrared Radiation Sounder
IASI	Infrared Atmospheric Sounding Interferometer
IFS	Integrated Forecasting System
IR	Infrared
JMA	Japan Meteorological Agency
MTSAT-1R	Multi-functional Transport Satellite-1 Replacement
NOAA	National Oceanographic and Atmospheric Administration
RMS	Root Mean Square forecast error
RTTOV	Radiative Transfer for TOV
SEVIRI	Spinning Enhanced Visible and Infrared Imager
WV	Water vapour